GEOPHYSICAL RESEARCH LETTERS, VOL. 25, NO. 20, PAGES 3867-3870, OCTOBER 15, 1998

Effects of 1997-1998 El Niño on tropospheric ozone and water vapor

S. Chandra[1], J.R. Ziemke[2], W. Min[3] and W. G. Read[4]

Abstract. This paper analyzes the impact of the 1997-1998 El Niño on tropospheric column ozone and tropospheric water vapor derived respectively from the Total Ozone Mapping Spectrometer (TOMS) on Earth Probe and the Microwave Limb Scanning instrument on the Upper Atmosphere Research Satellite. The 1997-1998 El Niño, characterized by an anomalous increase in sea-surface temperature (SST) across the eastern and central tropical Pacific Ocean, is one of the strongest El Niño Southern Oscillation (ENSO) events of the century, comparable in magnitude to the 1982-1983 episode. The major impact of the SST change has been the shift in the convection pattern from the western to the eastern Pacific affecting the response of rain-producing cumulonimbus. As a result, there has been a significant increase in rainfall over the eastern Pacific and a decrease over the western Pacific and Indonesia. The dryness in the Indonesian region has contributed to large-scale burning by uncontrolled wildfires in the tropical rainforests of Sumatra and Borneo. Our study shows that tropospheric column ozone decreased by 4-8 Dobson units (DU) in the eastern Pacific and increased by about 10-20 DU in the western Pacific largely as a result of the eastward shift of the tropical convective activity as inferred from National Oceanic and Atmospheric Administration (NOAA) outgoing longwave radiation (OLR) data. The effect of this shift is also evident in the upper tropospheric water vapor mixing ratio which varies inversely as ozone (O_3). These conclusions are qualitatively consistent with the changes in atmospheric circulation derived from zonal and vertical wind data obtained from the Goddard Earth Observing System data assimilation analyses. The changes in tropospheric column O_3 during the course of the 1997-1998 El Niño appear to be caused by a combination of large-scale circulation processes associated with the shift in the tropical convection pattern and surface/boundary layer processes associated with forest fires in the Indonesian region.

Introduction

Recently, *Ziemke et al.* [1998] have derived tropospheric column ozone (TCO) at tropical latitudes from Nimbus-7 and Earth Probe (EP) Total Ozone Mapping Spectrometer (TOMS) instruments using the convective cloud differential (CCD) technique. These data cover a period of about 19 years from 1979 to the present time with a gap of about three years after the demise of Nimbus-7 TOMS in May 1993 and launching of EP TOMS in July 1996. The tropospheric ozone data complement recently archived data on tropospheric H_2O in studying the transport characteristics of the tropical troposphere. The latter is derived from the Microwave Limb Sounding (MLS) instrument on the Upper Atmosphere Research Satellite (UARS) and covers a period of about 7 years from September 1991 to the present time. Both tropospheric ozone and H_2O are affected by changes in sea surface temperature (SST) [e.g., *Shiotani and Hasebe*, 1994; *Newell et al.*, 1997; *Ziemke et al.*, 1998]. For example, *Ziemke et al.* [1998] have shown that in the eastern Pacific TCO is strongly correlated with the El Niño Southern Oscillation (ENSO) showing a sharp decrease during El Niño events. *Newell et al.*[1997] showed that the temporal variations of upper tropospheric H_2O in the tropical equatorial region are closely correlated with the sea surface temperature changes in the eastern Pacific. In addition, *Kley et al.* [1996, 1997] have shown that ozone (O_3) and H_2O profiles measured during the Central Equatorial Pacific Experiment (CEPEX) are strongly influenced by changes in the convective pattern of the equatorial Pacific. In general, O_3 and H_2O are negatively correlated with low (high) O_3 and high (low) humidity in regions of enhanced (suppressed) convection.

The 1997-1998 El Niño has provided a unique opportunity for studying the role of convective transport over the entire tropical region. This ENSO event, characterized by an anomalous increase in SST across the eastern and central tropical Pacific Ocean, is one of the strongest of the century, comparable in magnitude to the 1982-1983 episode. The El Niño began to develop in March 1997 and has strengthened rapidly since then. Though the peak values of SST in the eastern Pacific Ocean occurred during October 1997, the El Niño has remained fairly robust through the end of 1997 with no sign of weakening in early 1998. The major impact of the SST change has been a shift in the convection pattern from the western to the eastern Pacific. As a result there has been a significant increase in rainfall over the eastern Pacific and decrease over the western Pacific and Indonesia. The dryness in the Indonesian region has contributed to large-scale burning by uncontrolled wildfires in the tropical rainforests of Sumatra and Borneo.

The purpose of this paper is to study the changes in convective patterns in the tropical atmosphere during the 1997-1998 El Niño and their effects on TCO and tropospheric H_2O. TCO is derived from the EP TOMS measurements using the CCD technique as discussed in *Ziemke et al.* [1998]. This technique uses high-density footprint measurements of TOMS total column O_3 and reflectivity in regions of high tropopause-level cloud tops. Since TOMS measures column O_3 only above cloud heights, TCO can be calculated by measuring the stratospheric component in the regions of high reflecting clouds and subtracting it from the total column measured from nearby low-reflecting or clear-sky regions. Comparisons with ozonesonde profiles in the tropics [*Ziemke and Chandra*, 1998] indicate that the primary contribution to TCO lies in the low to middle troposphere, maximizing around altitudes 4-5 km (~500 hPa).

The MLS instrument measures H_2O at 203 Ghz when the radiometer used to monitor stratospheric ClO is scanned down through the troposphere [*Read et al.*, 1995]. The data used in this paper are H_2O mixing ratio at 215 hPa (~12 km) derived from a preliminary retrieval. Convective activity is inferred using outgoing longwave radiation (OLR) flux measured from the National Oceanic and Atmospheric Administration (NOAA) polar orbiting satellites [*Liebmann and Smith*, 1996]. OLR is the amount of radiative flux (units W m^{-2}) re-emitted back to space in

[1]Code 916: NASA Goddard Space Flight Center
[2]Software Corporation of America
[3]General Science Corporation
[4]W. G. Read, Jet Propulsion Laboratory

Paper number 98GL02695.
0094-8276/98/98GL-02695$05.00

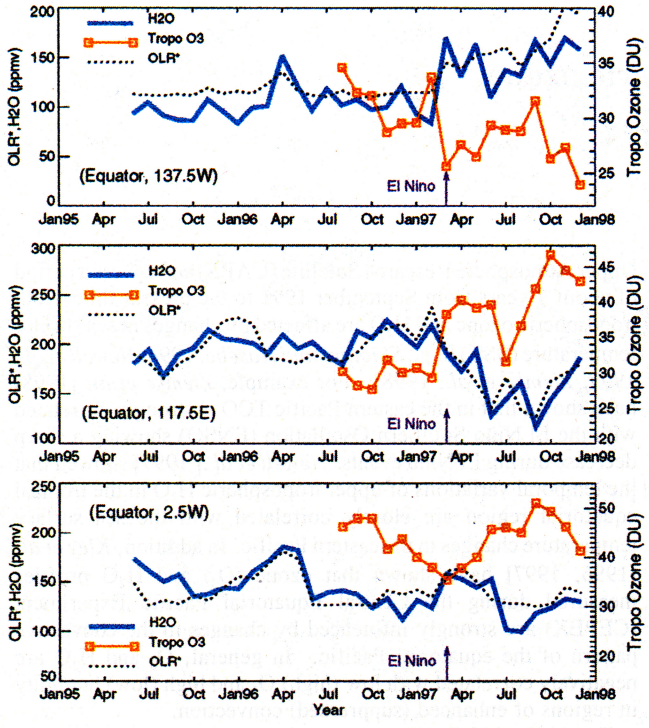

Figure 1. Monthly mean time series of UARS 215 hPa MLS H_2O volume mixing ratio (bold blue curve), EP TOMS TCO (red boxes), and NOAA adjusted OLR (dotted) from January 1979 through December 1997. OLR data have been scaled to that of MLS H_2O using the linear regression relationship OLR*=C0+C1*OLR where C0 and C1 are constants. Units for H_2O and OLR* are parts per million by volume. TCO measurements are in Dobson units. (top) Data centered at Equator, 137.5°W with C0=434, C1=-1.16. (middle) Data centered at Equator, 117.5°E with C0=390, C1=-0.93. (bottom) Data centered at Equator, 2.5°W with C0=460, C1=-1.25.

the 3.55-3.91 micron wavelength band and represents a measurement of convective activity. Low (high) values for OLR indicate the presence of strong (weak) convection.

Impact of convection on tropospheric O_3 and H_2O

Figure 1 shows temporal changes in MLS-derived H_2O mixing ratio at 215 hPa and the OLR* flux from January 1995 to December 1997 in the tropics at three selected longitudes in the eastern Pacific (top), western Pacific (middle), and Atlantic (bottom) regions. For visual comparison OLR flux has been scaled to that of MLS H_2O using a linear relationship OLR*=C0-C1*OLR (constants C0 and C1 are listed in the Figure 1 caption). This transformation makes OLR* to be inversely proportional to OLR so that an increase in OLR*(decrease in OLR) reflects an increase in convective activity and vice versa. Shown in this figure are also the corresponding changes in TCO from July 1996 derived from the EP TOMS measurements using the CCD technique [*Ziemke et al.*, 1998]. Unfortunately, O_3 data after the loss of Nimbus-7 TOMS in May 1993 and until the launch of EP TOMS in July 1996 are not available for comparison with the MLS H_2O data during this period. Figure 1 shows relatively small fluctuations in H_2O and OLR* both in the eastern Pacific (top) and the western Pacific (middle) until the beginning of El Niño in March 1997 when H_2O began a rapid ascent in the eastern Pacific, and fall in the western Pacific in phase with OLR*. Column O_3 in both of these regions also changes in concert with changes in OLR* though in the opposite direction. In comparison, OLR* does not show a significant trend in the Atlantic region (bottom) during the El Niño episode. Although the record is somewhat short, H_2O in this region shows a relatively stronger annual cycle with H_2O and O_3 varying in phase and out of phase respectively. The annual cycle in TCO shows an increase of 10-15 DU from a minimum of about 35 DU in March-April to a maximum of about 45-50 DU in September and October. This increase from the so called dry season to the wet season in Brazil and southern Africa is usually attributed to O_3 precursors (NO_x, CO, and hydrocarbons) produced as a result of biomass burning in the dry season [e.g., *Fishman et al.*, 1996; *Jacob et al.*, 1996; *Thomson et al.*, 1996 and references therein]. Figure 1 suggests that seasonal variations in both H_2O and O_3 in the troposphere are affected by seasonal variations in convective activity, which in turn are affected by changes in sea surface temperature [*Newell et al.*, 1997].

Figure 2 shows zonal anomalies (October 1997 minus October 1996) in TCO (top), upper-tropospheric H_2O (middle), and outgoing long-wave radiation (OLR, bottom) as a result of the shift of the normally-occurring strong convection in the tropical western Pacific region (i.e., west of longitude 180°) eastward into the tropical eastern Pacific. Compared to October 1996, TCO (top) in October 1997 decreased by 4-8 DU throughout much of the eastern Pacific and increased by about 10-20 DU in the western Pacific. This asymmetrical change with respect to the dateline is also present in both MLS 215 hPa upper-tropospheric H_2O (middle) and OLR (bottom) which are respectively out of phase and in-phase with O_3 variations. The enhanced convection in the eastern Pacific during El Niño resulted in an increase of 10-30 ppmv in H_2O with respect to 1996 values which were in the range of around 100 ppmv (see Figure 1). In the tropical western Pacific the effect was reversed as a result of suppressed convection. The upper tropospheric H_2O decreased by about 30-50 ppmv compared to 1996 values which were in the range of 200-225 ppmv. It may be noted that the percentage change in

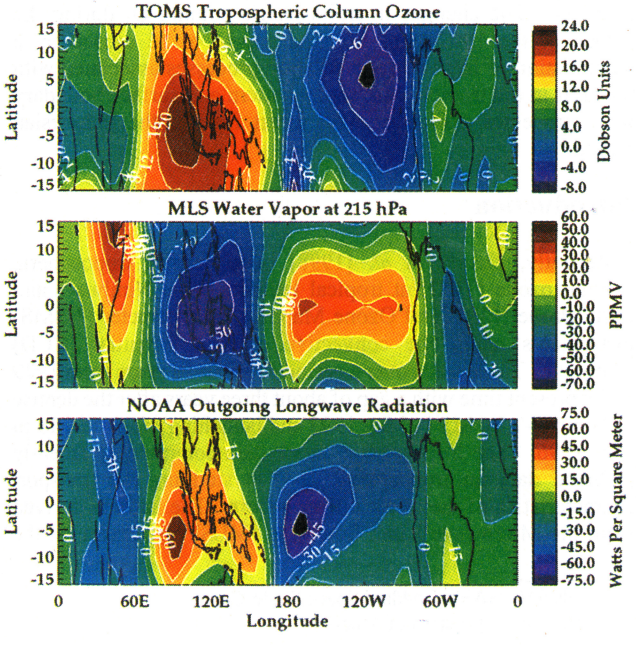

Figure 2. Tropical anomalies showing the effects of El Niño versus non-El Niño years for October months. Anomalies were computed by subtracting October 1996 monthly-mean data from that of October 1997. (top) EP TOMS CCD TCO (DU). (middle) MLS 215 hPa H_2O volume mixing ratio (units parts per million by volume). (bottom) NOAA OLR (units W m^{-2}).

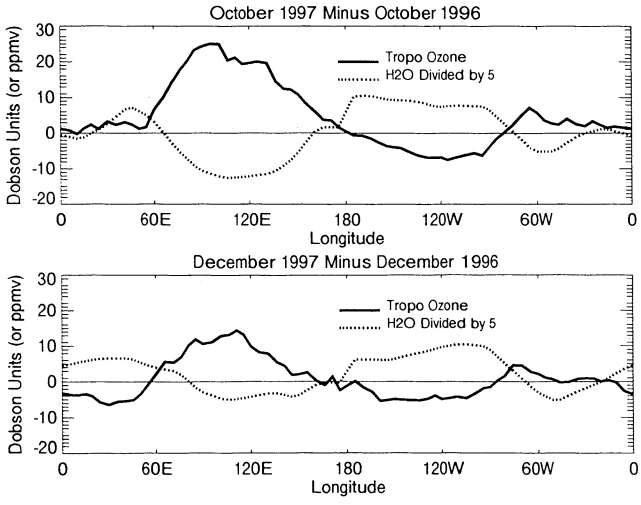

Figure 3. Tropical (5° S) zonal anomalies in TCO and H_2O in (top) October 1997 and (bottom) December 1997 with respect to the corresponding months in 1996.

TCO is larger than the corresponding percentage changes in H_2O and OLR. For example, a 10-20 DU increase in TCO in the western Pacific represents about 30-50% increase from 1996 whereas corresponding changes in both H_2O and OLR are around 20% of their respective 1996 means.

The El Niño induced changes in TCO, tropospheric H_2O, and OLR from August 1997 to December 1997 with respect to corresponding months in 1996 are similar to Figure 2. They appear like an asymmetrical dipole centered near the date line with O_3 in phase and H_2O out of phase with OLR. Figure 3 compares relative changes in TCO and H_2O for October and December months. It clearly shows the asymmetrical nature of O_3 and H_2O anomalies in the tropical Pacific with respect to the dateline. Similar asymmetry is also present in OLR data (not shown) which is in phase with TCO. The El Niño related changes in TCO are less apparent in the Atlantic region, encompassing equatorial regions of the continents of South America and Africa. The El Niño effects, in general, are weaker in this region compared to the Pacific as inferred earlier from Figure 1.

TCO derived from the Nimbus-7 TOMS data during the El Niño of 1982-1983 shows a decrease of about 4-8 DU in the eastern Pacific [Ziemke et al., 1998] and an increase of about the same magnitude in the western Pacific with respect to 14 years of Nimbus-7 climatology (figure not shown). These changes are consistent with El Niño-induced changes in OLR during this period. Unfortunately, satellite-based data for H_2O are not available for the 1982-1983 period to study the relative variability of TCO and H_2O. When calibration differences between Nimbus-7 and EP TOMS are taken into account, the 1997 changes in TCO with respect to the 14 years of Nimbus-7 TCO climatology are essentially similar to Figure 2. Both 1982-1983 and 1997-1998 events show comparable decrease in TCO (~4-8 DU) in the eastern Pacific. However, the increase in TCO during 1982-1983 period is about a factor of two smaller than the corresponding increase during 1997. It is interesting to note that during the 1982-1983 El Niño, an increase of 2-3 DU in the tropical western Pacific could be detected from the Nimbus-7 TOMS data even in the lowermost part of the troposphere (< 2.5 km) [*Kim and Newchurch*, 1998].

Implications from GEOS-1 data

The El Niño-related changes in TCO and H_2O can be qualitatively explained in terms of changes in the circulation pattern as illustrated in Figure 4 which shows pressure-longitude vector diagrams of zonal and vertical velocity along with specific humidity. The data in Figure 4 were obtained from the Goddard Earth Observing System (GEOS-1) data assimilation system [*Schubert et al.*, 1993]. These data were averaged monthly over 10°S-10°N for October 1996 (top), October 1997 (middle) and their 1997 minus 1996 difference (bottom). The dominant zonal structure in vertical wind during October 1996 appears like a classic Walker circulation [*Webster*, 1983] with a rising motion over Indonesia and the western Pacific and sinking motion east and west of this region. The middle panel in Figure 4 suggests a shift in circulation pattern in October 1997. The motion in October 1997 relative to October 1996 is predominantly downward in the western Pacific and Indonesian region, and upward in the eastern Pacific covering most of the area from the dateline eastward to the coast of Peru in south America. Figure 4 also shows changes in relative humidity from pre-El Niño to El Niño conditions. In both cases the humidity is maximum near the surface and decreases exponentially with altitude. The zonal changes in tropospheric water vapor in October 1997 with respect to October 1996 (Figure 4, bottom panel) are remarkably similar to changes inferred from the MLS H_2O data (Figure 2, middle panel) at 215 hPa and are consistent with the circulation pattern inferred from GEOS-1 data. Since the source of H_2O is primarily oceanic, upward motion associated with strong convection brings moist air into the middle and upper troposphere causing H_2O mixing ratio to increase. This effect is reversed when there is suppressed convection and/or downward motion.

Unfortunately, O_3 profiles from GEOS-1 simulation are not currently available for comparing with TOMS-derived TCO. About half the contribution to tropical TCO comes from the region below 6 km [e.g., *Ziemke et al.*, 1996] where H_2O is the main source of O_3 loss with a time constant of about a week [e.g., *Kley et al.*, 1996]. Typically, O_3 volume mixing ratio in the tropical Pacific region increases slowly from low values of 10-20 ppbv in the boundary layer to around 30-40 ppbv at about 5 km altitude. The upward

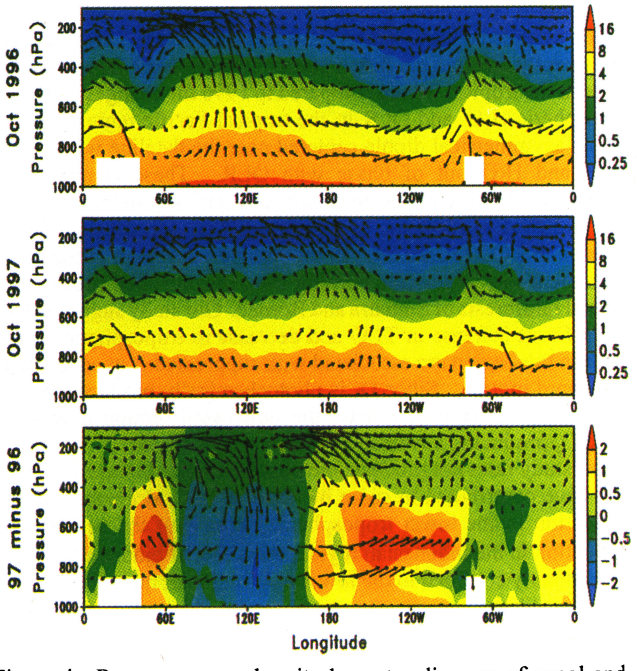

Figure 4. Pressure versus longitude vector diagram of zonal and vertical velocity, and specific humidity averaged over the 10°S-10°N latitudinal band from GEOS-1 analyses. (top) October 1996. (middle) October 1997. (bottom) Difference of October 1997 minus October 1996. The scaling factor between the zonal and vertical velocity is about 1000. Specific humidity (right-hand color bars) is in units g kg^{-1}.

motion will advect low O_3 and high H_2O upward and then, on a time scale of 1 week, the high H_2O values might produce additional O_3 reduction. This process is reversed when the motion is downward. Since O_3 is photochemically produced in the middle and the upper troposphere [e.g., *Jacob et al.*, 1996] the downward motion may also cause the O_3-producing air mass to increase in regions of suppressed convection.

We note from Figures 1-3 that the regions of enhanced O_3 over Indonesia also coincide with the regions of intense biomass burning in southeast Asia that occurred during the very dry months of September and October. The EP TOMS instrument has detected smoke from the Indonesian fires from early September to the middle of November 1997 (http://jwocky.gsfc.nasa.gov/indonesia.html). It may be argued that the increase in TCO in the Indonesian region is caused by O_3 precursors (NO_x, CO, and hydrocarbons) produced as a result of biomass burning during this period. Like H_2O, the transport of these precursors into the middle and the upper troposphere is likely to be inhibited because of suppressed convection in this region. The effect of biomass burning is therefore likely to be confined to the lowermost part of the troposphere near the boundary layer.

Kim and Newchurch [1998] have estimated a seasonal excursion of 2-4 DU over an annual mean of about 7 DU in lower tropospheric O_3 (at altitudes < 2.5 km), over the western Pacific Ocean near New Guinea. They attribute this excursion to biomass burning during the dry northern summer-spring months (July-September). The estimate of seasonal excursion by *Kim and Newchuch* [1998] is based on climatological values and may be significantly greater for specific events such as the Indonesian fires of 1997. One may therefore reasonably conclude that the observed changes in TCO during 1997-1998 El Niño are manifestations of large-scale circulation and surface/boundary layer processes.

Summary and conclusions

The 1997-1998 El Niño episode has produced a major shift in the atmospheric convective pattern from the western to the eastern Pacific as inferred from NOAA OLR measurements. This shift has significantly affected the distribution of tropospheric O_3 and water vapor in the tropics. When compared to 1996 the changes in TCO, tropospheric H_2O, and OLR in the tropical Pacific region appear like an asymmetrical dipole centered near the dateline with O_3 in phase and H_2O out of phase with OLR. These changes are consistent with the circulation pattern as inferred from the GEOS-1 data. Relative to 1996, the El Niño in 1997 produced a significant increase in TCO (10-20 DU) in the Indonesian region at the time when there was large-scale burning from uncontrolled fires in the tropical rainforests of Sumatra and Borneo. Our study suggests that a significant increase in TCO and decrease in tropospheric water vapor in this region are associated with suppressed convection and downward motion. Since O_3 is photochemically produced in the middle and upper troposphere, the downward motion may also cause O_3 producing airmass to increase in this region.

Our study does not preclude the possibility that Indonesian fires may have contributed to some increase in TCO as a result of O_3 production in the lower troposphere. Because of the suppressed convection in the Indonesian region, the effect of biomass burning was probably confined to the lowermost region of the troposphere. The most likely scenario for the observed changes in TCO is a combination of large scale circulation and surface/boundary layer processes.

Acknowledgments. We thank P. K. Bhartia, Mark Schoeberl, Siegfried Schubert, and Anne Thompson for their helpful comments on the manuscript. We also thank Mike Newchurch for valuable comments and suggestions. The OLR data used in this paper were provided by NOAA/Climate Prediction Center via Internet.

References

Fishman, et al., The NASA GTE TRACE A Experiment (Septembr-October 1992): Overview, *J. Geophys. Res., 101*, 23,865-23,879, 1996.

Jacob et al., Origin of ozone and NO_x in the tropical troposphere: A photochemical analysis of aircraft observations over the South Atlantic basin, *J. Geophys. Res., 101*, 24,235-24250, 1996.

Kim, J. H., and M. J. Newchurch, Biomass-burning influence on tropospheric ozone over New Guinea and South America, *J. Geophys. Res., 103*, 1455-1461, 1998.

Kley et al., Observations of near-ozone concentrations over the convective Pacific: Effects on air chemistry, *Science, 274*, 230-233, 1996.

Kley et al., Tropospheric water vapor and ozone cross-sections in a zonal plane over the central equatorial Pacific Ocean, *Q. J. R. Meteorol. Soc., 123*, 2009-2040, 1997.

Liebmann, B., and C. A. Smith, Description of a complete (interpolated) outgoing longwave radiation dataset, *Bull. Am. Meteorol. Soc., 77*, 1275-1277, 1996.

Newell, R. E., Y. Zhu, W. G. Read, and J. W. Waters, Relationship between tropical tropospheric moisture and eastern tropical Pacific sea surface temperature at seasonal and inter-annual time scales, *Geophys. Res. Lett., 24*, 25-28, 1997.

Read et al., Upper-Tropospheric H_2O from UARS MLS, *Bull. Am. Meteorol. Soc., 76*, 2381-2389, 1995.

Schubert, S., D. J. Pfaendtner, R. Rood, An assimilated data set for Earth Science applications, *Bull. Am. Meteorol. Soc., 74*, 2331-2342, 1993.

Shiotani, M., and F. Hasebe, Stratospheric ozone variations in the equatorial region as seen in Stratospheric Aerosol and Gas Experiment data, *J. Geophys. Res., 99*, 14,575-14,584, 1994.

Thompson,et al., Where did tropospheric ozone over southern Africa and the tropical Atlantic come from in October 1992? Insights from TOMS, GTE/TRACE-A and SAFARI-92, *J. Geophys. Res., 101*, 24,251-24,278, 1996.

Webster, P., Large-scale structure of the tropical atmosphere, Large-Scale Dynamical Processes in the Atmosphere, B. Hoskins and R. Pierce (Eds.), *Academic Press*, 235-276., 1983.

Ziemke, J. R., S. Chandra, A. M. Thompson, and D. P. McNamara, Zonal asymmetries in southern hemisphere column ozone: Implications of biomass burning, *J. Geophys. Res., 101*, 14,421-14427, 1996.

Ziemke, J. R., S. Chandra, and P. K. Bhartia, Two new methods for deriving tropospheric column ozone from TOMS measurements: The assimilated UARS MLS/HALOE and convective-cloud differential techniques, *J. Geophys. Res., 103*, in press, 1998.

Ziemke, J. R., and S. Chandra, On tropospheric ozone and the tropical wave 1 in total ozone, *Proceedings of the XVIII Quadrennial Ozone Symposium*, L' Aquilla, Italy 12-21 September, 1996, edited by R. D. Bojkov and Giido Visconti, 1, 447-450, 1998.

S. Chandra, Code 916, NASA Goddard Space Flight Center, Greenbelt, MD 20771 (e-mail: chandra@chapman, gsfc.nasa.gov)

J. R. Ziemke, Software Corporation of America, Lanham, MD 20706

W. Min, General Science Corporation, Laurel, MD 20707

W. G. Read, Jet Propulsion Laboratory, Pasadena, CA 91109

(Received April 8, 1998; revised July 16, 1998;
accepted August 13, 1998.)